Magnetoresistance of Antiphase Boundaries in Sr$_2$FeMoO$_{6-\delta}$

Gunnar Suchaneck* and Evgenii Artiukh

Antiphase boundaries (APB) in strontium ferromolybdate induce antiferro-magnetically coupled spins of the Fe ions at the boundary affecting both the magnetic properties and the electron transport across the boundary. Herein, first, 3D presentation of the APB in strontium ferromolybdate is presented. For the first time, the weighted antiferromagnetic (AF) modulus, the bulk ferrimagnetic exchange stiffness constant, and the AF exchange stiffness constant across the APB of strontium ferromolybdate are estimated. This is done by analyzing carefully selected experimental data of the magnetoresistance (MR). The boundary width and boundary energy are calculated by means of Kittel's theory of the structure of ferromagnetic domains in films and small particles. The evaluation of these parameters deepens the understanding of MR in strontium ferromolybdate ceramic and thin-film samples possessing a high density of APBs.

1. Introduction

Strontium ferromolybdate (Sr$_2$FeMoO$_{6-\delta}$—SFMO) is the most studied ferrimagnetic (FM) double perovskite. SFMO double perovskites are promising candidates for magnetic electrode materials for room-temperature spintronics applications, because they present a half-metallic character (with theoretically 100% polarization), a high Curie temperature (T_C) of about 415 K (ferromagnets should be operated in their ordered magnetic state below T_C), and a low-field magnetoresistance (LFMR).[1] However, a wide application of SFMO is still missing, because of the low reproducibility of its magnetic properties originating in antisite and antiphase boundary (APB) defect formation, oxygen stoichiometry, and aging in contact with air and moisture.[2]

G. Suchaneck
Solid State Electronics Laboratory
TU Dresden
01062 Dresden, Germany
E-mail: gunnar.suchaneck@tu-dresden.de

E. Artiukh
Cryogenic Research Division
SSPA "Scientific-Practical Materials Research Centre of NAS of Belarus"
220072 Minsk, Belarus

The ORCID identification number(s) for the author(s) of this article can be found under https://doi.org/10.1002/pssb.202100353.

In SFMO, the dominating point defects are Fe and Mo antisite defects, that is, by Fe atoms on Mo sites, Fe$_{Mo}$, and vice versa, Mo$_{Fe}$.[2] This antisite disorder (ASD) gives rise to neighboring Fe—O—Fe regions and, thus, to the formation of APBs.[3] APBs promote antiferromagnetic (AF) superexchange interactions.[4] The alignment of the AF spins at the APB with the external magnetic field changes the electron conductivity across the AF boundaries, leading to a large MR.

In general, APBs are characterized by a crystallographic shear vector describing the relative displacement of the two parts of the crystal on either side of the interface. They were first obtained 60 years ago in a Fe$_3$Al superlattice.[5] As neighbor-like bonds occur across APBs, the possibility of trapping and recombination of charge carriers as well as charge scattering arises in III−V and II−VI compound semiconductors.[6] In group III−V semiconductors, the formation of APBs hinders the growth of high-quality wafers in achieving high-performance solar cells and nonlinear optical integrations.[7] A close relationship between the electrical properties and the stacking sequence at the interface density of APBs was found in superconducting YBa$_2$Cu$_3$O$_{7-\delta}$ thin films deposited by pulsed laser deposition onto SrTiO$_3$ substrates.[8] Experimentally, a correlation between electronic transport properties and the presence of meandering APBs within insulating charge ordered domains was obtained in the certain perovskite Nb$_{0.5}$Sr$_{0.5}$MnO$_3$.[9] This was interpreted as the existence of metallic regions forming around APBs. AF behavior of APBs was first studied in magnetite (Fe$_3$O$_4$) epitaxial thin films grown on (100) MgO substrates.[10] Here, APBs affect magnetization at high field and, consequently, the approach to magnetic saturation.[11] A model of spin-polarized transport across the APBs in Fe$_3$O$_4$(001) thin films has been developed to explain the dependence of the electrical resistance and intrinsic MR on film thickness.[12] The model predicts an electrical conductivity along a hard magnetization axis quadratically changing with a magnetic field until it equals the anisotropy field and an approximately linear change for higher fields. In contrast, single magnetite crystals without AF-APBs do not show any MR.[13]

The existence of APBs in Sr$_{2-x}$Ca$_x$FeMoO$_6$ ceramics was proposed in the study by Goodenough et al.[14] to explain the shape of the $M-H$ hysteresis loops below the Curie temperature T_C, where M is the magnetization and H is the magnetic field strength; a small coercivity and the appearance of low remanence are also seen. APBs in SFMO ceramics were observed for the first time by high-resolution transmission electron microscopy

(HRTEM) in the study by Navarro et al.[3] The dimensions of the antiphase domains were estimated to be of the order of 0.5 μm. Another HRTEM study revealed the presence of APBs inside Mo-rich grains of SFMO samples with Sr- and Fe-rich grain boundaries.[15] These samples exhibit typical properties characteristic of the presence of APBs and increased B-site disorder: a lower saturation magnetization, higher resistivity, lower coercivity, and higher LFMR. HRTEM of Ba_2FeMoO_6[16] and X-ray diffraction and X-ray absorption fine structure experiments of SFMO give evidence that a high degree of short-range order is preserved even in samples with high ASD. Here, the size of the antiphase domains amounts to only $0.8-1.5$ nm which increases with ASD.[17] The conjunction of locally ordered regions forms magnetic nanodomains.[3,16] Thereby, the segregation of antisite defects leads to the creation of APBs,[17] which coincide perfectly with the nanodomain boundary.[16] The predicted for Fe_3O_4 linear field dependence of MR at high magnetic fields was experimentally proved in SFMO samples annealed at 900 °C.[18,19] With increasing annealing temperature, the domains increase in size, exhibit increasing ordering, and the linear contribution to MR decreases up to an annealing temperature of 1500 °C, where the conventional tunneling MR (TMR) completely takes over. Note that the classical LFMR of SFMO is practically absent in samples annealed at 900 °C, whereas above 1100 °C, a TMR-like low-field response starts to become visible. Thus, the APB mechanism of the MR should be valid for ceramics synthesized or postannealed in the temperature region $900 °C < T < 1500 °C$ but with a fraction decreasing with temperature. Another subject is (111)-textured SFMO thin films which were deposited onto (111) $SrTiO_3$ or (111) Pt on platinized Si wafers. Here, the present APB has a superstructure direction aligned with the growth direction.[20] MR attributed to the tunneling across APBs was obtained in epitaxial SFMO films grown by pulsed laser deposition in an oxidizing atmosphere.[21] An additional indication of the presence of APBs in these films was the insufficient saturation of the magnetic moment at a field of 1 T.

As a result, APBs are very well characterized in Fe_3O_4. For SFMO, there is clear experimental evidence of APB presence and indications of impact on physical properties, but physical parameters of these types of structural defects are still missing.

Therefore, the aim of this article is the estimation of the parameters determining the MR of APBs in SFMO (weighted AF modulus, bulk FM exchange stiffness constant, and AF exchange stiffness constant across the APB) as a base for the application of SFMO-based magnetic sensors using the change of resistance of APBs.

2. Structure and Magnetic Properties of APBs in SFMO

SFMO possesses a tetragonal structure with the *I4/m* space symmetry group.[22] The perfect SFMO lattice structure consists of corner-connected FeO_6 and MoO_6 octahedra alternating along the three axes. The Sr cations are in the voids formed by FeO_6 and MoO_6 octahedra. The Fe and Mo ions form a rock salt-type cation order at the perovskite B-site (**Figure 1**a).

APBs are natural growth defects arising between two coherent crystallites facing each other, with stacking of FeO_6 and MoO_6 octahedra starting from the opposite cation. For instance, during thin-film growth, islands may merge at the boundaries which are mutually rotated or translated by a fraction of the unit cell.[23] Other origins of APBs are terraces or steps on the surfaces of the substrate.[24] In ceramics, APBs remain as relics of grain boundaries after prolonged annealing at intermediate temperatures around 900 °C.[18] Antiphase stacking forms planes of either strongly AF Fe—O—Fe (Figure 1b) or weakly magnetic Mo—O—Mo bonds. The two planes nearest to the APB layers are supposed to have a small B-site disorder. Their Mo and Fe ions couple ferrimagnetically. APBs locally interrupt FM coupling between Fe and Mo ions and the indirect Fe—O—Mo—O—iron exchange interaction occurring in defect-free structures, leading to new magnetic exchange interactions, which are not present in the bulk material. Without an external magnetic field, the resistance across the AF APB would be large. When the external field is applied, the AF spins in the APB would be rotated progressively to the orientation of the external field. The electron current transport across the APB increases as the external field increases. At high enough magnetic fields, antiferromagnetically coupled spins at the AFB align perpendicular to
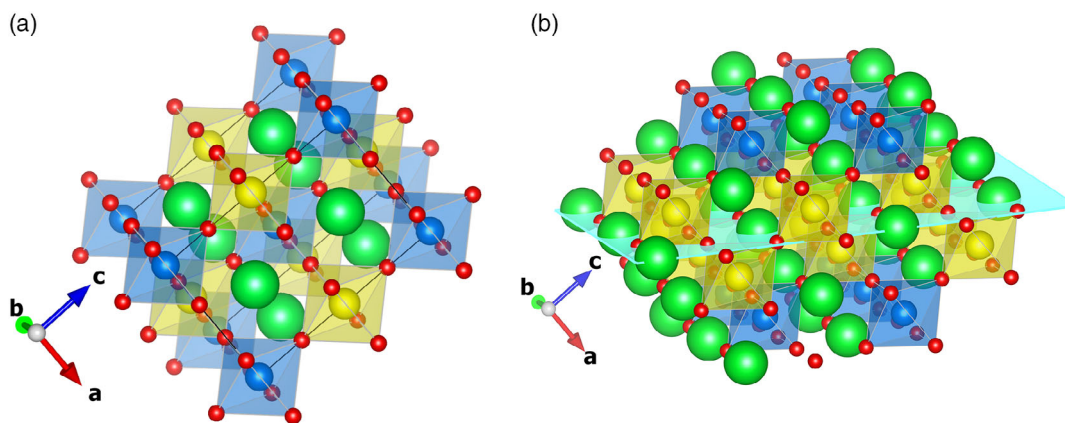

Figure 1. a) Ideal lattice structure of SFMO and b) SFMO lattice with an APB. Strontium ions are green, iron ions yellow, molybdenum ions blue, and oxygen ions red. These images were drawn using the 3D visualization program for structural models, VESTA.[41]

the applied field and do not contribute to the magnetization. This hinders the saturation of magnetization. If the volumes of the two different crystallites were not equal, there would be a residual magnetization on reducing the field to zero from the saturation value. The residual magnetization would give rise to a finite but small remanence.[14] The formation of Mo—O—Mo bonds is of minor importance for magnetic properties, because of the only weak magnetic coupling between the two Mo spins.

3. Spin Chain Model for Spin-Polarized Transport Across an AF Boundary

In a 1D model of two half-ferromagnetic linear chains AF coupled at the APB,[12] the conductivity σ_{AF} across the APB is proportional to $\cos^2\varphi_{AF}$, where φ_{AF} is the angle between the spins on either side of the boundary. The model considers an atomically sharp interface, it takes only axial anisotropy into account, and it presupposes that the angle φ_{AF} is close to $\pi/2$. At zero magnetic field, AF coupling across the APB blocks the conductivity. On application of a magnetic field, the angle φ_{AF} deviates from π (**Figure 2**) and the conductivity across the sheet becomes significant. For external magnetic flux densities B, σ_{AF} in perpendicular MR geometries is, depending on the uniaxial anisotropy value B_{an}, given by[12]

$$\sigma_{AF} \propto \cos^2\varphi = \frac{(M_s B)^2}{4KW_{AF}} \tag{1}$$

for $B < B_{an}$ and

$$\sigma_{AF} \propto \cos^2\varphi_{AF} = \frac{M_s B - K}{W_{AF}} \tag{2}$$

for $B > B_{an}$, where M_s is the saturation magnetization, K the magnetocrystalline anisotropy constant, $W_{AF} = A^2{}_{AF}/A_F x^2$ the weighted AF modulus, A_F the bulk FM exchange stiffness constant, A_{AF} the AF exchange stiffness constant across the APB, and x the distance between two neighboring AF-coupled spin chains across the APB. In the case of SFMO, B_{an} is about 0.1 T.[25]

The total electrical conductivity then consists of an APB-independent contribution σ_0 and an AF contribution σ_{AF} due to the presence of APBs. The MR is then given by
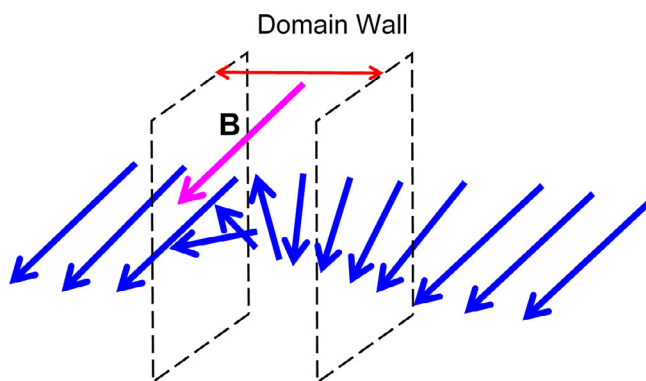

Figure 2. Spin orientation across an atomically sharp APB with AF coupling on application of a magnetic field.

$$MR = \frac{\rho(B) - \rho(0)}{\rho(0)} = -\left(\frac{\sigma_0}{\sigma_{AF}} + 1\right)^{-1} \tag{3}$$

where ρ is the resistivity. For small σ_{AF}, $\sigma_{AF} \ll \sigma_0$. This yields a linear dependence of the MR on σ_{AF}.

$$MR \simeq -C \cdot \frac{(M_s B)^2}{4KW_{AF}} \tag{4}$$

and

$$MR \simeq -C \cdot \frac{M_s B - K}{W_{AF}} \tag{5}$$

respectively. Here, the proportionality factor C depends on the volume fraction of APBs in the film and is thus expected to increase with increasing APB density. A linear behavior of the MR above a magnetic flux density of 1.5 T, at least up to of 7 T, is characteristic for SFMO comprising nanosized domains, as they are much more difficult to being magnetized along the direction of the magnetic field.[18] In contrast, the MR of Fe_3O_4 follows the expression.[26]

$$MR \simeq -C\left[\frac{M_s B}{W_{AF}} - \left(\frac{M_s B}{W_{AF}}\right)^{3/2}\right] \tag{6}$$

already at $B > 1$ T.

4. Results and Discussion

The parameters of Equation (4) and (5) were derived from MR data of SFMO ceramics measured up to a magnetic flux density of 7 T.[18] **Figure 3** illustrates the fitted curves in relation to experiments. The parameters obtained for SFMO are compiled in **Table 1** in comparison with Fe_3O_4 and the corresponding references to Fe_3O_4 data. Note that the weighted AF modulus W_{AF} can be estimated only within a factor of C. In the case of $Fe_3O_4(111)$, the proportionality factor C, fit to the more precise Equation (6), decreased from about 56 to 38 with a thickness d increasing from
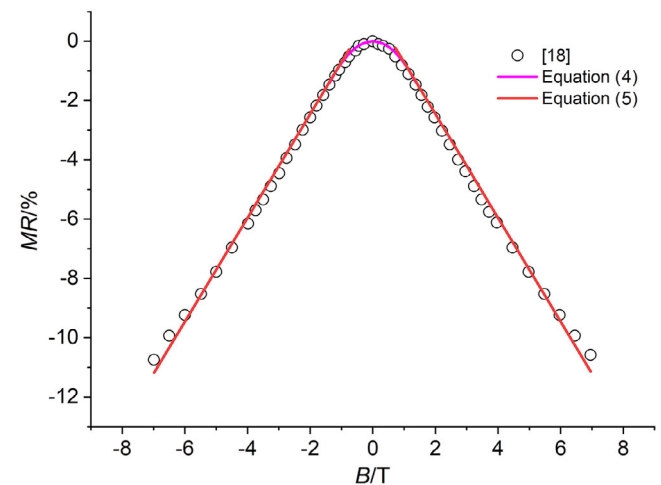

Figure 3. MR at 5 K depending on magnetic flux densities. Circles: experiment[18] and solid lines: fit.

Table 1. Parameters of the MR of APBs in SFMO compared with the ones of Fe_3O_4.

	Sr_2FeMoO_6	Fe_3O_4	Ref.
M_s [μ_B f.u.$^{-1}$]	3.8$^{a)}$	4.1	[27]
W_{AF} [J m^{-3}]	$C \cdot 1.63 \times 10^5$	3.76×10^6	[10]
		1.12×10^7	[26]
K [J m^{-3}]	1.70×10^5	1.3×10^4	[42]
		1.3×10^4	[27]
		1.36×10^4	[43]
A_{AF} [J m^{-1}]	$8.33 \times 10^{-13b)}$	2.14×10^{-11}	[44]
		9.215×10^{-12}	[45]
		1.12×10^{-11}	[46]
		1.19×10^{-11}	[27]
		1.19×10^{-11}	[45]
		1.32×10^{-11}	[43]
		10^{-13}, TF(110)	[37]
		2.36×10^{-11}	[47]
A_F [J m^{-1}]	$2.35 \times 10^{-11}/C$	1.527×10^{-12}	[46]
		7.0×10^{-12}	[45]

$^{a)}$Ref. [18]; $^{b)}$estimated based on the $Fe^{3+}-O-Fe^{3+}$ exchange constant J^S_{180} taken from the study by Motida et al.[44]

5 to 50 nm.[26] Thereby, the product $C \cdot M_s/W_{AF}$ is a function slowly changing with film thickness and decreasing exponentially from a value of about 2 for $d \to 0$ to about 1.2 for $d = 2 \mu m$. Here, ultrathin films thinner than 5 nm show paramagnetic behavior.[27]

An anisotropy constant $K = 2.74 \times 10^4$ J m^{-3} was determined for SFMO thin films by ferromagnetic resonance at room temperature.[25] In contrast, we have deduced K from the correction to the Mössbauer hyperfine field given in the case of uniaxially symmetric particles by[28]

$$B_{obs} \approx B_{hf}\left(1 - \frac{kT}{2KV}\right) \qquad (7)$$

where B_{obs} is the observed magnetic hyperfine field at the temperature T and B_{hf} is the static magnetic hyperfine field. For an experimental shift of $B_{obs}/B_{hf} = 0.55$ at $T = 298$ K,[29] this results in $KV = 4.6 \times 10^{-21}$ J and, correspondingly, to $K = 2.26 \times 10^4$ J m^{-3}. Furthermore, the classical theory of the temperature dependence of the magnetic anisotropy constant K predicts a value of $K(T)/K(0) \approx 0.16$ for iron at $T/T_C = 0.7$.[30] Here, K diminishes less than 20% up to $T/T_C = 0.3$, that is, $K(T < 0.3T_C) \approx K(0)$. Extrapolating the above given SFMO value at $T/T_C = 0.7$ back, we obtain $K(0) = 1.7 \times 10^5$ J m^{-3}, as cited in Table 1. This value is in satisfactory agreement with magnetocrystalline anisotropic energies $E(001) - E(011) \approx -27 \mu eV \cdot f.u.^{-1}$ (-7.7×10^4 J m^{-3}) and $E(001) - E(111) \approx -67 \mu eV \cdot f.u.^{-1}$ (-1.7×10^5 J m^{-3}) calculated by means of first principles.[31]

The experimental value of A_F for ferromagnetic metals, $BaFe_{12}O_{19}$, $SmCo_5$, and $Nd_2Fe_{14}B$ is of the order of

$A_F \approx 1.0 \times 10^{-11}$ J m^{-1}.[32] An estimation of the value A_F using the spin-wave stiffness D[33] is given by

$$A_F(T) = \frac{D(T)M_s(T)}{2g\mu_B} \qquad (8)$$

The values of D available for SFMO were derived from a fit to a $T^{3/2}$ term of the specific heat in the temperature range $5-100$ K.[34,35] For purpose of definiteness, we attribute them to a temperature of 50 K. This yields a value $A_F(50$ K$) = 1.85 \times 10^{-12}$ J m^{-1} for the low-temperature region supposing $M_s(0) = 3.8 \mu_B \cdot f.u.^{-1}$ The temperature dependencies $D(T)$ and $M_s(T)$ then determine $A_F(T)$. For magnetite, the reduced magnetization $m = M(T)/M(0)$ scales as a power law $A_F \propto m^\alpha$ with $\alpha = 1.7$.[33] Later, the power law exponents were redefined to be $\alpha = 1.66$, 1.715, and 1.745 for simple cubic, body-centered cubic, and face-centered lattices, respectively.[36] With regard to the SFMO room-temperature value of the reduced magnetization $m \approx 0.67$,[1] we obtain $A_F(300$ K$) \approx 9.2 \times 10^{-13}$ J m^{-1} for the case of two interpenetrating face-centered cubic sublattices, suggesting a value of C in the order of 25.

For SFMO thin films, experimental data of the influence of APBs on the electrical conductivity are scarce. The authors[21] claim tunneling across APBs in pulsed-laser-deposited SFMO thin films. Fitting the linear part of the magnetic field dependence of the MR in this report to Equation (5), we obtain a weighted AF modulus of $W_{AF} = C \cdot 4.1 \times 10^6$ J m^{-3} when keeping all other data constant. This is in accordance with Fe_3O_4 thin films, where the average exchange stiffness constant A_{AF} is much lower than that in bulk ceramics.[27,37]

Kittel derived a square root relationship between the magnetic domain stripe width w and film thickness d.[38] This relationship holds also for APBs, for instance, in magnetite.[39,40] Both the boundary energy γ_w and the boundary width δ_w are related to the antiferroelectric exchange stiffness A_{AF} and the magnetocrystalline anisotropy constant K:[32]

$$\gamma_w = 4 \cdot (K \cdot A_{AF})^{1/2} \qquad (9)$$

$$\delta_w = \pi \cdot \left(\frac{A_{AF}}{K}\right)^{1/2} \qquad (10)$$

which we have derived from MR as described. This allows us to make estimations of their values, yielding a domain wall energy of 1.51 mJ m^{-2} and a domain wall thickness of 7.0 nm.

5. Conclusion

APBs appear in SFMO ceramics and thin films fabricated under special synthesis conditions. Using the spin chain model, developed for magnetite comprising APBs, the bulk FM exchange stiffness constant and the AF exchange stiffness constant across the APB of SFMO were estimated by means of experimental data of MR. As APBs coincide with domain boundaries, the boundary energy and boundary width were derived based on Kittel's magnetic domain strip theory. The physical values obtained in this work enable the design of magnetic sensors based on the resistance change of APBs.

Conflict of Interest

The authors declare no conflict of interest.

Data Availability Statement

The data that support the findings of this study are available from the corresponding author upon reasonable request.

[1] K. I. Kobayashi, T. Kimura, H. Sawada, K. Terakura, Y. Tokura, *Nature* **1998**, *395*, 677.

[2] G. Suchaneck, N. Kalanda, E. Artsiukh, G. Gerlach, *Phys. Status Solidi B* **2020**, *257*, 1900312.

[3] J. Navarro, L. Balcells, F. Sandiumenge, M. Bibes, A. Roig, B. Martínez, J. Fontcuberta, *J. Phys. Condens. Matter.* **2001**, *13*, 8481.

[4] D. Sánchez, J. A. Alonso, M. García-Hernández, M. J. Martínez-Lope, J. L. Martínez, A. Mellergård, *Phys. Rev. B: Condens. Matter Mater. Phys.* **2002**, *65*, 104426.

[5] M. J. Marcinkowski, N. Brown, *J. Appl. Phys.* **1962**, *33*, 537.

[6] D. B. Holt, *J. Phys. Chem. Solids* **1969**, *30*, 1297.

[7] A. C. Lin, M. M. Fejer, J. S. Harris, *J. Cryst. Growth* **2013**, *363*, 258.

[8] G. Rijnders, S. Currás, M. Huijben, D. H. A. Blank, H. Rogalla, *Appl. Phys. Lett.* **2004**, *84*, 1150.

[9] N. Fukumoto, S. Mori, N. Yamamoto, Y. Moritomo, T. Katsufuji, C. H. Chen, S.-W. Cheong, *Phys. Rev. B: Condens. Matter Mater. Phys.* **1999**, *60*, 12963.

[10] D. T. Margulies, F. T. Parker, M. L. Rudee, F. E. Spada, J. N. Chapman, P. R. Aitchison, A. E. Berkowitz, *Phys. Rev. Lett.* **1997**, *79*, 5162.

[11] J. B. Moussy, S. Gota, A. Bataille, M. J. Guittet, M. Gautier-Soyer, F. Delille, B. Dieny, F. Ott, T. D. Doan, P. Warin, P. Bayle-Guillemaud, C. Gatel, E. Snoeck, *Phys. Rev. B: Condens. Matter Mater. Phys.* **2004**, *70*, 174448.

[12] W. Eerenstein, T. T. M. Palstra, S. S. Saxena, T. Hibma, *Phys. Rev. Lett.* **2002**, *88*, 247204.

[13] J. M. D. Coey, A. E. Berkowitz, L. Balcells, F. F. Putris, F. T. Parker, *Appl. Phys. Lett.* **1998**, *72*, 734.

[14] J. B. Goodenough, R. I. Dass, *Int. J. Inorg. Mater.* **2000**, *2*, 3.

[15] T. T. Fang, *Phys. Rev. B: Condens. Matter Mater. Phys.* **2005**, *71*, 064401.

[16] T. Asaka, X. Z. Yu, Y. Tomioka, Y. Kaneko, T. Nagai, K. Kimoto, K. Ishizuka, Y. Tokura, Y. Matsui, *Phys. Rev. B: Condens. Matter Mater. Phys.* **2007**, *75*, 184440.

[17] C. Meneghini, S. Ray, F. Liscio, F. Bardelli, S. Mobilio, D. D. Sarma, *Phys. Rev. Lett.* **2009**, *103*, 046403.

[18] A. Nag, S. Jana, S. Middey, S. Ray, *IOP Conf. Ser. Mater. Sci. Eng.* **2013**, *46*, 012001.

[19] A. Nag, S. Jana, S. Middey, S. Ray, *Indian J. Phys.* **2017**, *91*, 883.

[20] T. Manako, M. Izumi, Y. Konishi, K. I. Kobayashi, M. Kawasaki, Y. Tokura, *Appl. Phys. Lett.* **1999**, *74*, 2215.

[21] A. Venimadhav, F. Sher, J. P. Attfield, M. G. Blamire, *J. Magn. Magn. Mater.* **2004**, *269*, 101.

[22] Y. C. Hu, J. J. Ge, Q. Ji, B. Lv, X. S. Wu, G. F. Cheng, *Powder Diffr.* **2010**, *25*, S17.

[23] S. Celotto, W. Eerenstein, T. Hibma, *Eur. Phys. J. B* **2003**, *36*, 271.

[24] S. K. Arora, R. G. S. Sofin, I. V. Shvets, *Phys. Rev. B: Condens. Matter Mater. Phys.* **2005**, *72*, 134404.

[25] T. Nosach, G. Mullady, N. Leifer, V. Adyam, Q. Li, S. Greenbaum, Y. Ren, *J. Appl. Phys.* **2008**, *103*, 07E311.

[26] A. V. Ramos, J. B. Moussy, M. J. Guittet, A. M. Bataille, M. Gautier-Soyer, M. Viret, C. Gatel, P. Bayle-Guillemaud, E. Snoeck, *J. Appl. Phys.* **2006**, *100*, 103902.

[27] F. Voogt, T. Palstra, L. Niesen, O. Rogojanu, M. James, T. Hibma, *Phys. Rev. B: Condens. Matter Mater. Phys.* **1998**, *57*, R8107(R).

[28] S. Mørup, *J. Magn. Magn. Mater.* **1983**, *37*, 39.

[29] T. Nakagawa, *J. Phys. Soc. Jpn.* **1968**, *24*, 806.

[30] C. Zener, *Phys. Rev.* **1954**, *96*, 1335.

[31] X. Chen, D. Parker, K. P. Ong, M.-H. Du, D. J. Singh, *Appl. Phys. Lett.* **2013**, *102*, 102403.

[32] R. Skomski, in *Spin Electronics* (Eds.: M. Ziese, M. J. Thornton), Lecture Notes in Physics, Vol. 569, Springer, Berlin, Heidelberg **2001**.

[33] F. Heider, W. Williams, *Geophys. Res. Lett.* **1988**, *15*, 184.

[34] Y. Tomioka, T. Okuda, Y. Okimoto, R. Kumai, K. Kobayashi, Y. Tokura, *Phys. Rev. B: Condens. Matter Mater. Phys.* **2000**, *61*, 422.

[35] Y. Moritomo, S. Xu, T. Akimoto, A. Machida, N. Hamada, K. Ohoyama, E. Nishibori, M. Takata, M. Sakata, *Phys. Rev. B: Condens. Matter Mater. Phys.* **2000**, *62*, 14224.

[36] U. Atxitia, D. Hinzke, O. Chubykalo-Fesenko, U. Nowak, H. Kachkachi, O. N. Mryasov, R. F. Evans, R. W. Chantrell, *Phys. Rev. B: Condens. Matter Mater. Phys.* **2010**, *82*, 134440.

[37] Q. Pan, T. G. Pokhil, B. M. Moskowitz, *J. Appl. Phys.* **2002**, *91*, 5945.

[38] C. Kittel, *Phys. Rev.* **1946**, *70*, 965.

[39] W. Eerenstein, T. T. M. Palstra, T. Hibma, S. Celotto, *Phys. Rev. B: Condens. Matter Mater. Phys.* **2002**, *66*, 201101(R).

[40] A. M. Bataille, L. Ponson, S. Gota, L. Barbier, D. Bonamy, M. Gautier-Soyer, C. Gatel, E. Snoeck, *Phys. Rev. B: Condens. Matter Mater. Phys.* **2006**, *74*, 155438.

[41] K. Momma, F. Izumi, *J. Appl. Crystallogr.* **2011**, *44*, 1272.

[42] E. J. Fletcher, W. O'Reilly, *J. Phys. C: Solid State Phys.* **1974**, *7*, 171.

[43] H. C. Wu, S. K. Arora, O. N. Mryasov, I. V. Shvets, *Appl. Phys. Lett.* **2008**, *92*, 182502.

[44] K. Motida, S. Miyahara, *J. Phys. Soc. Jpn.* **1970**, *28*, 1188.

[45] P. J. Van Der Zaag, A. R. Ball, L. F. Feiner, R. M. Wolf, P. A. A. Van Der Heijden, *J. Appl. Phys.* **1996**, *79*, 5103.

[46] E. De Grave, R. M. Persoons, R. E. Vandenberghe, P. M. A. De Bakker, *Phys. Rev. B* **1993**, *47*, 5881.

[47] H. C. Wu, M. Abid, B. S. Chun, R. Ramos, O. N. Mryasov, I. V. Shvets, *Nano Lett.* **2010**, *10*, 1132.